Integrating High DER-Penetrated Distribution Systems into ISO Energy Market Clearing: A Feasible Region Projection Approach

Yikui Liu, Student Member, IEEE, Lei Wu, Senior Member, IEEE, Yonghong Chen, Senior Member, IEEE, Jie Li, Member, IEEE,

Abstract-Primary distribution systems are usually simplified as fixed or flexible loads in the Independent System Operator (ISO) energy market clearing with favorable computational features. However, in emerging distribution systems with an increasing penetration of distributed energy resources (DER), this simplifycation could easily fail to capture economic features of DERs and internal limits of distribution systems, triggering line congestion and under/over-voltage issues. To this end, a feasible region projection-based approach is proposed in this paper to optimally integrate high DER-penetrated distribution systems into the ISO energy market clearing, while effectively capturing configuration details of distribution systems and fully respecting their internal physical limits such as voltage and line flow constraints. Numerical studies show efficacy of the proposed approach in achieving the optimal integration of high DER-penetrated distribution systems into the ISO energy market, while: (i) not requiring ISO directly formulating full distribution systems with exhaustive variables and constraints; and (ii) not necessitating an iterative procedure to interact ISO with distribution systems, thus compatible to the current ISO market practice.

Index Terms—Distributed energy resources, distribution system integration, energy market, feasible region projection.

NOMENCLATURE

Index of distribution systems.

Index of fixed loads.

Indices:

d

g	Index of units/DERs.
h	Index of generated constraints.
i, i', i''	Index of buses.
i - i'	Index of lines, from bus i to bus i' .
ref	Index of the reference bus.
t, t'	Index of hours.
Sets:	
\mathcal{D}	Set of distribution systems.
$\mathcal{oldsymbol{D}}_{(i)}$	Set of distribution systems that contain bus i
	as an interconnection bus.
\mathcal{F}^T	Set of fixed loads in the transmission system.
$oldsymbol{\mathcal{F}}_d^D$	Set of fixed loads in distribution system <i>d</i> .
$oldsymbol{\mathcal{F}}_d^D \ oldsymbol{\mathcal{F}}_i^T$	Set of fixed loads connected at bus i in the
	transmission system.
$oldsymbol{\mathcal{F}}_{i,d}^{\scriptscriptstyle D}$	Set of fixed loads connected at bus i in

This work was supported in part by the U.S. National Science Foundation grants CNS-1915756 and ECCS-1952683.

distribution system d.

Disclaimer: The views expressed in this paper are solely those of the authors and do not necessarily represent those of MISO.

${m G}^T$	Set of units in the transmission system.			
$oldsymbol{\mathcal{G}}_d^{\scriptscriptstyle D}$	Set of DERs in distribution system <i>d</i> .			
$oldsymbol{\mathcal{G}}_{i}^{T}$	Set of units connected at bus i in the			
\mathcal{J}_{l}	transmission system.			
$oldsymbol{\mathcal{G}}_{i.d.}^{D}$	Set of DERs connected at bus i in distribution			
$9_{i,d}$				
	system d.			
$oldsymbol{\mathcal{H}}_{d,t}$	Set of generated constraints for distribution			
	system d at hour t .			
${m {\mathcal J}}^T$	Set of buses in transmission system.			
$oldsymbol{\mathcal{I}}_d^{\scriptscriptstyle D}$	Set of buses in distribution system <i>d</i> .			
$oldsymbol{\mathcal{J}}_d^B$	Set of duplicated interconnection buses in			
u	distribution system d .			
$oldsymbol{\mathcal{J}}_{i,d}^T$	The counterpart of an interconnection bus $i \in$			
-,	\mathcal{J}_d^B in the transmission system.			
\mathcal{L}^T	Set of lines in the transmission system.			
\mathcal{L}_d^D	Set of lines in distribution system <i>d</i> .			
$oldsymbol{\mathcal{T}}^{"}$	Set of hours in the scheduling time horizon,			
	$T \triangleq \{1,2\}.$			

Variables for the Transmission System:

$\hat{l}_{g,t}$	Binary indicator of ON/OFF status of unit g at
_	hour t.
$\hat{p}_{g,t}$	Active power dispatch of unit g at hour t .
$\hat{p}_{i-i',t}$	Active power flow on line $i - i'$ at hour t .
$\hat{p}_{i,d,t}$	Active power injection to distribution system
	d from interconnection bus i at hour t .
$\widehat{Y}_{g,t}$	Binary indicator of startup action of unit g at
_	hour t.
$\hat{Z}_{g,t}$	Binary indicator of shutdown action of unit g
<i>5</i> ,	at hour t.
$\widehat{ heta}_{i,t}$	Voltage phase angle of bus i at hour t .
$\widehat{ heta}_{i,t}$ $\widehat{ heta}_{ref,t}$	Voltage phase angle of the reference bus at
- , ,-	hour $t, ref \in \mathcal{J}^T$.

Parameters for the Transmission System:

Parameters for the Transmission System:					
$\hat{\mathcal{C}}_g$	Bidding price of unit g .				
$\widehat{\mathit{CL}}_g$	No-load cost of unit g .				
$\widehat{P}_{f,t}$	Active power demand of fixed load f at hour t .				
\hat{P}_{i-i}^{UB}	Power flow limit of line $i - i'$.				
$\widehat{P}_g^{LB}/\widehat{P}_g^{UB}$	Active power lower/upper bound of unit g .				
$\widehat{R}_g^{RU}/\widehat{R}_g^{RD}$	Ramp-up/down ability of unit g during				
	operation procedure.				
$\widehat{R}_g^{SU}/\widehat{R}_g^{SD}$	Ramp-up/down ability of unit g during				
	startup/shutdown procedure.				
\widehat{SU}_g	Startup cost of unit g .				
$\widehat{SF}_{i-i',i''}$	Shift factor of bus i'' to line $i - i'$.				
\widehat{TU}_g	Minimum ON time of unit g .				

Y. Liu and L. Wu are with ECE Department, Stevens Institute of Technology, Hoboken, NJ, 07030 USA. (E-mail: yliu262, lei.wu@stevens.edu). Y. Chen is with Midcontinent ISO, Carmel, IN, 46032 USA. J. Li is with ECE Department, Rowan University, Glassboro, NJ, 08028 USA.

\widehat{TD}_g	Minimum OFF time of unit g .
$\hat{X}_{i-i'}$	Reactance of line $i - i'$.

Variables for the Distribution System:

$I_{g,t}$	Binary indicator of ON/OFF status of DER g
	at hour t .
$p_{i-i',t}$	Active power flow along line $i - i'$ at hour t .
$p_{g,t}$	Active power dispatch of DER g at hour t .
$p_{i,t}$	Net active power injection from the transmission system through interconnection
	bus i at hour t .
$q_{i-i',t}$	Reactive power flow along line $i - i'$ at hour
	t.
$q_{g,t}$	Reactive power dispatch of DER g at hour t .
$q_{i,t}$	Net reactive power injection from the transmission system through interconnection bus i at hour t .
$v_{i.t}$	Voltage magnitude of bus i at hour t .
$Y_{g,t}$	Binary indicator of startup action of DER g at
	hour t.
$ heta_{i,t}$	Voltage phase angle of bus i at hour t .

Parameters for the Distribution System:

$A_{h,i,t}^{\theta}, A_{h,i,t}^{P}$	Coefficients in generated constraint h to bus i
$^{11}h,i,t,$ $^{11}h,i,t$	at hour t.
$A_{h,g,t}^G, A_{h,g,t}^I$	
$A_{h,g,t}, A_{h,g,t}$	Coefficients in generated constraint h to DER
	g at hour t.
$B_{h,t}$	Right-hand-side of generated constraint h at
	hour t.
$B_{i-i'}$	Susceptance of line $i - i'$.
C_g	Bidding price of DER g .
CL_g	No-load cost of DER g .
$G_{i-i'}$	Conductance of line $i - i'$.
P_{i-i}^{UB}	Power flow limit of line $i - i'$.
$P_{f,t}$	Active power demand of fixed load f at hour t .
P_i^{UB}	Bound of net active power injection from the
	transmission system through interconnection
	bus i.
P_g^{LB}/P_g^{UB}	Active power lower/upper bound of DER g .
$Q_{f,t}$	Reactive power demand of fixed load f at
,,	hour t.
Q_i^{UB}	Bound of net reactive power injection from the
	transmission system through interconnection
	bus i.
Q_g^{LB}/Q_g^{UB}	Reactive power lower/upper bound of DER g .
	Startup cost of DER g .
SU_g	-
V_i^{LB}/V_i^{UB}	Voltage magnitude lower/upper limit of bus i .

I. Introduction

TN recent years, electric energy generation from distributed energy resources (DER), especially renewable DERs such as solar and wind, keeps increasing and has reached a considerable share in the electric energy sector [1]-[2]. To this end, DERs have been reforming power flow patterns of distribution systems, transforming distribution line flows from unidirectional to multidirectional. In addition, a high penetration of renewables is usually accompanied with an increased level of loads [3], because of electricity price reduction in wholesale energy market. Thus, combining the two factors, line congestions in distribution systems would be more likely to happen [4], which is rarely observed in passive distribution systems of the past. Moreover, because of high resistance-to-reactance ratios of distribution lines, bus voltages in distribution systems are also sensitive to active power injections from DERs, and a deeper penetration of DERs could trigger voltage rise issues [5].

However, in the recent efforts in promoting DER integration in Independent System Operators (ISO) markets, DERs are only allowed to bid on interconnection buses between transmission and distribution systems. Indeed, in most ISO energy markets, primary distribution systems are usually simplified as fixed loads with forecasted values or flexible loads with aggregated bids, while DERs resided in the distribution systems are merely considered as behind-themeter load modifiers [6]. Consequently, DER dispatch instructions from the ISO market clearing results, which neglect bus voltage and line flow limits of distribution networks, could potentially cause voltage violations, line flow congestions, and even forced curtailment of renewable energy.

In current bulk energy market practice, ISOs do not collect configuration details, such as DER and network data, to exhaustively model primary distribution systems. Thus, to optimally integrate DER-penetrated distribution systems into bulk energy market operation, extensive efforts are needed in the near future to promote data sharing through timely communications between the ISO and distribution system operators (DSO). However, even in such a future scenario, the ISO may still be reluctant to directly model distribution systems with exhaustive details, which usually requires a complex AC power flow model with a significant number of extra variables to capture internal operation constraints, such as voltage and line flow limits. Therefore, to tackle this obstacle, a compact distribution system model is desired to accurately capture the relationship between ISO-DSO active power exchange and active power outputs of individual DERs, while effectively capturing DER economic features and fully respecting internal operation limits of distribution systems.

Several models and mechanisms have been proposed in literature [7]-[16] to study the coordinated operation of transmission system and DER-penetrated distribution systems. Reference [7] reviewed the current practice in ISO-DSO coordination with proliferated DERs, and indicated that a certain level of preliminary coordination could be achieved through tailored market mechanisms and rules. More complex market designs were reviewed in [8] and thereafter. In the academic field, bilevel models represent a mainstream approach for ISO-DSO coordination [9]-[11]. Specifically, [9] proposed a bilevel ISO-DSO coordination framework, in which the ISO clears the energy market in an upper level, and individual DSOs optimize their consumptions with respect to ISO energy market clearing prices in a lower level and in turn

impact the ISO market clearing results. This framework is further extended to study other problems while considering various economic and physical characters of the distribution network. For instance, electric energy procurement of DSOs was discussed in [12] to coordinate heterogeneous DERs, for minimizing the total distribution system operation cost while securing financial targets of individual DERs. Reference [13] proposed to manage DERs and other assets coordinately within a two-phase model. However, although bilevel models free the ISO from acquiring configuration details of distribution systems, these models are usually solved via an iterative procedure, which may be hard to be adopted by ISOs at the current stage because of the concerns on coordination ability, policies, and operation platform upgrade.

In comparison, [14]-[16] discussed approaches to approximate distribution systems in the ISO energy market, which could be practical applicable to the current ISO market framework. References [14]-[15] adopted univariate linear functions to describe the relationship between operating costs and net power injections of distribution systems. Reference [16] depicted the feasible region of net power injections while considering operation constraints of distribution systems. However, [14]-[16] assume that primary distribution systems are connected to the transmission system through a single interconnection bus, that is, power exchange between distribution and transmission systems solely depends on net load of the distribution system. In reality, primary distribution systems, especially those in urban areas, are usually connected to the transmission system via multiple interconnection buses for enhancing power supply reliability. Under this situation, power injections at multiple interconnection buses are electrically coupled, depending on line impedances and generation dispatches both inside and outside the distribution system. Consequently, ISO-DSO coordination models in references [14]-[16] would become invalid.

Targeting on primary distribution systems connected to the transmission system via multiple interconnection buses, this paper discusses an approach to integrate DER-penetrated distribution systems into the ISO energy market. First, we formulate the feasible operation region of a distribution system, described by physical limits such as bus voltage and line flow constraints. Then, we categorize variables of the feasible region into desired and undesired ones, and apply a feasible region projection approach to eliminate undesired variables while preserving desired ones. Finally, the desired variables and their associated constraints are included in the ISO energy market model, which can capture impacts of distribution systems in the transmission system while respecting economic features of DERs as well as internal physical limits of distribution systems.

The proposed approach stands from the perspective of ISOs and pays special attention to practical applicability potentials in the current ISO energy market platform. Specifically, it resolves the main obstacle of existing practice on simplified distribution systems (i.e., fixed or flexible loads), which cannot fully respect internal operation constraints of distribution systems. In addition, this approach does not

require iterative interaction between the ISO and DSOs, and presents promising computational advantages as compared to directly modeling the full distribution systems exhaustively.

The rest of the paper is organized as follows. The ISO day-ahead energy market model and the feasible operation region of distribution systems are presented in Section II. Section III discusses the integration of distribution systems into the ISO energy market. Section IV explores beneficial modeling features of a special situation, when each distribution system is connected to the transmission system via a single interconnection bus. Numerical case studies are conducted in Section IV, and the conclusions are drawn in Section V.

II. ISO ENERGY MARKET AND FEASIBLE OPERATION REGION OF DISTRIBUTION SYSTEMS

This paper considers radial/looped primary distribution systems that are connected to the transmission system through interconnection buses. Targeted systems are not directly modeled or monitored by ISOs, but simplified as a power injection/withdrawn point in the ISO energy market model. Their typical voltage levels could be 35kV and 12kV (i.e., only high voltage level distribution systems are considered). In fact, the proposed distribution system integration model can be extended to sub-transmission systems that are either not explicitly simulated by ISOs or expected to be benefited with a more detailed model for ensuring operation feasibility, especially voltage limitations.

Fig. 1 shows a looped distribution system connected to the transmission system through two interconnection buses. For the sake of formulation, we duplicate variables of interconnection buses to be used in distribution and transmission system models separately, as shown in Fig. 2. Fig. 2 also illustrate parts of sets and variables defined in the Nomenclature. $\hat{\cdot}$ indicates variables and parameters of the transmission system (e.g., $\hat{\theta}_{i,t}$), distinguishing from those of the distribution systems (e.g., $\theta_{i,t}$).

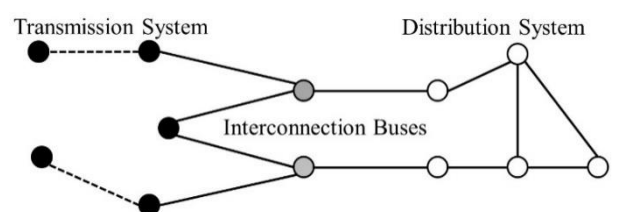


Fig. 1 An illustrative example of a distribution system connected to the transmission system with two interconnection buses

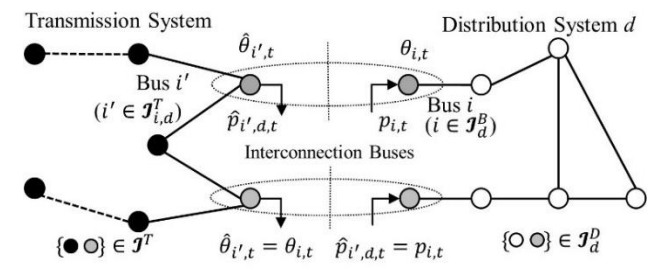


Fig. 2 Illustration of variable duplication

A. ISO Day-Ahead Energy Market Model

(13)

(25)

A light version of the ISO day-ahead energy market model (1)-(12) is used as a base to study the main focus of this paper. i.e., integrating DER-penetrated distribution systems into the ISO energy market. It considers thermal units only, and includes line flow limits at the system level as well as minimum ON/OFF time limits, dispatch ranges, and ramping limits at the unit level. The model can be extended to consider other types of system assets (such as flexible loads and virtual bids) and constraints (such as reserve limits).

The objective (1) of the ISO energy market is to minimize system operating cost, including energy cost, no-load cost, and startup cost. The DC power flow model (2)-(3) is formulated via the voltage phase angle form, assuming unity voltage magnitudes for all buses and ignoring reactive power flows. Active power flow on line i - i' at hour t is calculated as in (2) and restricted by the line flow limit by (4). Nodal active power balance is enforced by (3). Variable $\hat{\theta}_{i,t}$ and $\hat{p}_{i,d,t}$ in (3) are illustrated in Fig. 2. Constraint (5) limits dispatch ranges of units. Constraints (6)-(7) are the classic "3-bin" form startup/shutdown logic. Unit minimum ON and OFF time limits are enforced by (8)-(9). Constraints (10)-(11) represent unit ramp-up and down limits during operation procedure, as well as during startup and shutdown procedures. Constraint (12) assigns the reference bus.

$$\begin{aligned} \min \sum_{t \in \mathcal{T}} \sum_{g \in \mathcal{G}^T} (\hat{C}_g \cdot \hat{p}_{g,t} + \widehat{CL}_g \cdot \hat{I}_{g,t} + \widehat{SU}_g \cdot \hat{Y}_{g,t}) & (1) \\ \hat{p}_{i-i',t} &= (\hat{\theta}_{i,t} - \hat{\theta}_{i',t}) / \hat{X}_{i-i'}; & i - i' \in \mathcal{L}^T, t \in \mathcal{T} & (2) \\ \sum_{i-i' \in \mathcal{L}^T} \hat{p}_{i-i',t} + \sum_{d \in \mathcal{D}_{(i)}} \hat{p}_{i,d,t} + \sum_{f \in \mathcal{F}_i^T} \hat{P}_{f,t} & \\ &= \sum_{i'-i \in \mathcal{L}^T} \hat{p}_{i'-i,t} + \sum_{g \in \mathcal{G}_i^T} \hat{p}_{g,t}; & i \in \mathcal{J}^T, t \in \mathcal{T} & (3) \\ -\hat{P}_{i-i'}^{UB} &\leq \hat{p}_{i-i',t} \leq \hat{P}_{i-i'}^{UB}; & i - i' \in \mathcal{L}^T, t \in \mathcal{T} & (4) \\ \hat{P}_g^{LB} \cdot \hat{I}_{g,t} &\leq \hat{p}_{g,t} \leq \hat{P}_g^{UB} \cdot \hat{I}_{g,t}; & g \in \mathcal{G}^T, t \in \mathcal{T} & (5) \\ \hat{Y}_{g,t} - \hat{Z}_{g,t} &= \hat{I}_{g,t} - \hat{I}_{g,t-1}; & g \in \mathcal{G}^T, t \in \mathcal{T} & (6) \\ \hat{Y}_{g,t} + \hat{Z}_{g,t} &\leq 1; & g \in \mathcal{G}^T, t \in \mathcal{T} & (7) \\ \sum_{t'=t-TD_g+1}^t \hat{Y}_{g,t'} &\leq \hat{I}_{g,t}; & g \in \mathcal{G}^T, t \in \mathcal{T} & (8) \\ \sum_{t'=t-TD_g+1}^t \hat{Z}_{g,t'} &\leq 1 - \hat{I}_{g,t}; & g \in \mathcal{G}^T, t \in \mathcal{T} & (9) \\ \hat{p}_{g,t} - \hat{p}_{g,t-1} &\leq \hat{R}_g^{RU} \cdot \hat{I}_{g,t-1} + \hat{R}_g^{SU} \cdot \hat{Y}_{g,t}; & g \in \mathcal{G}^T, t \in \mathcal{T} & (10) \\ \hat{p}_{g,t-1} - \hat{p}_{g,t} &\leq \hat{R}_g^{RD} \cdot \hat{I}_{g,t} + \hat{R}_g^{SD} \cdot \hat{Z}_{g,t}; & g \in \mathcal{G}^T, t \in \mathcal{T} & (11) \\ \hat{\theta}_{ref,t} &= 0; & t \in \mathcal{T} & (12) \end{aligned}$$

B. Feasible Operation Region Model of Distribution Systems

In recognizing that ISOs usually adopt a linear model to ensure computational efficiency, it is desirable to also formulate the feasible operation region of distribution systems via linear models. To this end, we adopt an approximated linear power flow model [17] for distribution systems, given its advantages including: (i) considering voltage magnitudes and reactive power flow, (ii) no needs on initial operation point, and (iii) relatively high approximation accuracy.

The feasible operation region of distribution system d can be formulated as in (13)-(25). Active and reactive power flows along line i - i' at hour t are calculated as in (13)-(14). Nodal active and reactive power balance for internal and interconnection buses are respectively constrained by (15)-(16) and (17)-(18). Constraint (19) fixes voltage magnitudes of the interconnection buses as 1 p.u., being consistent with the

DC power flow-based transmission system model. Constraints (20) and (21) restrict line flows and bus voltages. Net active and reactive power injections from the transmission system are constrained as in (22) and (23). When $p_{i,t}/q_{i,t}$ is negative, distribution system d provides active/reactive power support to the transmission system. Dispatch ranges of DERs are limited by their active and reactive power bounds as in (24) and (25). We use \mathcal{P}_d to denote the feasible operation region (13)-(25) of distribution system d. $p_{i-i',t} = G_{i-i'} \cdot \left(v_{i,t} - v_{i',t}\right) - B_{i-i'} \cdot \left(\theta_{i,t} - \theta_{i',t}\right);$

$$\begin{aligned} p_{i-i',t} &= G_{i-i'} \cdot (v_{i,t} - v_{i',t}) - B_{i-i'} \cdot (\theta_{i,t} - \theta_{i',t}); \\ &\quad i - i' \in \mathcal{L}_d^D, t \in \mathcal{T} \quad (13) \\ q_{i-i',t} &= -B_{i-i'} \cdot (v_{i,t} - v_{i',t}) - G_{i-i'} \cdot (\theta_{i,t} - \theta_{i',t}); \\ &\quad i - i' \in \mathcal{L}_d^D, t \in \mathcal{T} \quad (14) \\ \sum_{i-i' \in \mathcal{L}_d^D} p_{i-i',t} + \sum_{f \in \mathcal{F}_{i,d}^D} P_{f,t} &= \sum_{i' - i \in \mathcal{L}_d^D} p_{i' - i,t} + \sum_{g \in \mathcal{G}_{i,d}^D} p_{g,t}; \\ &\quad i \in \mathcal{I}_d^D / \mathcal{I}_d^B, t \in \mathcal{T} \quad (15) \\ \sum_{i-i' \in \mathcal{L}_d^D} q_{i-i',t} + \sum_{f \in \mathcal{F}_{i,d}^D} Q_{f,t} &= \sum_{i' - i \in \mathcal{L}_d^D} q_{i' - i,t} + \sum_{g \in \mathcal{G}_{i,d}^D} q_{g,t}; \\ &\quad i \in \mathcal{I}_d^D / \mathcal{I}_d^B, t \in \mathcal{T} \quad (16) \\ \sum_{i-i' \in \mathcal{L}_d^D} p_{i-i',t} &= p_{i,t}; \quad i \in \mathcal{I}_d^B, t \in \mathcal{T} \quad (17) \\ \sum_{i-i' \in \mathcal{L}_d^D} q_{i-i',t} &= q_{i,t}; \quad i \in \mathcal{I}_d^B, t \in \mathcal{T} \quad (18) \\ v_{i,t} &= 1; \quad i \in \mathcal{I}_d^B, t \in \mathcal{T} \quad (19) \\ -P_{i-i'}^{UB} \leq p_{i-i',t} \leq P_{i-i'}^{UB}; \quad i - i' \in \mathcal{L}_d^D, t \in \mathcal{T} \quad (20) \\ V_i^{LB} \leq v_{i,t} \leq V_i^{UB}; \quad i \in \mathcal{I}_d^B, t \in \mathcal{T} \quad (21) \\ -P_i^{UB} \leq p_{i,t} \leq P_i^{UB}; \quad i \in \mathcal{I}_d^B, t \in \mathcal{T} \quad (22) \\ -Q_i^{UB} \leq q_{i,t} \leq Q_i^{UB}; \quad i \in \mathcal{I}_d^B, t \in \mathcal{T} \quad (23) \\ P_g^{LB} \leq p_{g,t} \leq P_g^{UB}; \quad g \in \mathcal{G}_d^D, t \in \mathcal{T} \quad (24) \\ Q_g^{LB} \leq q_{g,t} \leq Q_g^{UB}; \quad g \in \mathcal{G}_d^D, t \in \mathcal{T} \quad (25) \end{aligned}$$

III. INTEGRATING THE FEASIBLE OPERATION REGION OF DISTRIBUTION SYSTEMS INTO THE ISO ENERGY MARKET

 $g \in \mathcal{G}_d^D, t \in \mathcal{T}$

A. Feasible Region Projection Method

Feasible operation region \mathcal{P}_d contains extra variables beyond those used in the ISO energy market model, such as $v_{i,t}$ and $q_{g,t}$. To keep the consistency of the integration model with the ISO's current practice, and avoid those additional variables in \mathcal{P}_d being penetrated in the ISO energy market model, we eliminate these variables via the projection approach. Therefore, variables in the \mathcal{P}_d are classified into desired variables \mathcal{V}_d^D and undesired variables \mathcal{V}_d^U , where desired variables refer to the ones that will be included in the ISO energy market model, i.e., $\mathcal{V}_d^D = \{\theta_{i,t} \text{ and } p_{i,t}, \forall i \in \mathcal{V}_d^D \}$ \mathbf{J}_{d}^{B} ; $p_{g,t}$, and all other variables of $\mathbf{\mathcal{P}}_{d}$ are undesired variables and contained in \mathcal{V}_d^U .

The feasible operation region \mathcal{P}_d of distribution system d (13)-(25) can be represented in a compact form (26), where A_d^D and A_d^U are coefficient matrices of \mathcal{V}_d^D and \mathcal{V}_d^U , and B_d is a vector of constant terms. We note that equality constraints are not explicitly shown in (26), which can be equivalently represented as two inequality constraints.

$$\boldsymbol{A}_{d}^{D} \cdot \boldsymbol{\mathcal{V}}_{d}^{D} + \boldsymbol{A}_{d}^{U} \cdot \boldsymbol{\mathcal{V}}_{d}^{U} \le \boldsymbol{B}_{d} \tag{26}$$

We project the feasible region (26) onto the space of \mathcal{V}_d^D as in (27) [18]-[19]. The projection refers to that, if \mathcal{V}_d^D is a feasible solution to (27), there must exist \mathcal{V}_d^U such that \mathcal{V}_d^D and \mathcal{V}_d^U together is a feasible solution to (26). In (27), \mathcal{C}_d^D and \mathcal{D}_d are coefficient matrix and constant vector generated via the feasible region projection process.

$$\boldsymbol{C}_d^D \cdot \boldsymbol{\mathcal{V}}_d^D \le \boldsymbol{D}_d \tag{27}$$

Feasible region projection is realized with Gaussian elimination [18] and Fourier-Motzkin elimination [19] via two steps: (i) variables $p_{i-i',t}$ and $q_{i-i',t}$ are eliminated immediately by substituting equality constraints (13)-(14) in (15)-(18). After that, equality constraints (15)-(19) are used to further eliminate $\theta_{i,t}$ $(i \in \mathcal{J}_d^D/\mathcal{J}_d^B)$, $v_{i,t}$, and $q_{i,t}$, i.e., equality constraints are reformatted in a row echelon form by Gaussian elimination to substitute these variables in inequality constraints; (ii) Fourier-Motzkin elimination further processes remaining undesired variables $q_{g,t}$ in inequality constraints.

A well-recognized shortcoming of Fourier-Motzkin elimination is its exponential complexity in theory. We adopt the Imbert's acceleration theorems to mitigate the exponential growth of inequality constraints by filtering out redundant ones generated in each iteration, thereby accelerating the algorithm [19]. In fact, other effective but computationally more expensive filtering methods can also be embedded. Reference [20] discussed an effective mixed-integer linear programming (MILP) based iterative algorithm to identify constraints. Various redundant constraint redundant identification methods are reviewed in [21]. We adopt a linear programming (LP) method [21] to mitigate redundancy in each iteration of Fourier-Motzkin elimination. This step is referred to as the LP filtering in this paper.

The flowchart of the proposed feasible region projection process is shown in Fig. 3. Gaussian elimination is executed first to deal with part of undesired variables, after which remaining undesired variables will be further eliminated iteratively via Fourier-Motzkin elimination. In each Fourier-Motzkin elimination iteration, one variable is eliminated, and some constraints will be generated concomitantly; then LP filtering is implemented to filter out redundant constraints to maintain compactness of the formulation. Intuitively, the number of iterations is equal to the number of variables to be eliminated. The detained steps of Gaussian elimination and Fourier-Motzkin elimination can be referred to from references [18] and [19].

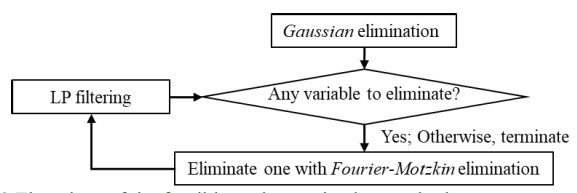


Fig. 3 Flowchart of the feasible region projection method

Finally, two facts of the feasible region projection of \mathcal{P}_d are emphasized: (i) Since no time-coupling constraints are presented in the feasible region (13)-(25), projections of \mathcal{P}_d for individual time periods can be conducted in parallel; (ii) Gaussian elimination and Fourier-Motzkin elimination only process constraints containing undesired variables, constraints (22) and (24) keep unchanged throughout the feasible region projection process.

B. Integrating the Feasible Operation Region of Distribution Systems into the ISO Energy Market

The feasible region projection method discussed above constructs a feasible region $\widetilde{\boldsymbol{\mathcal{P}}}_d$ for desired variables $\boldsymbol{\mathcal{V}}_d^D$ out of the original feasible region \mathcal{P}_d , guaranteeing that for any feasible solution $\mathcal{V}_d^D \in \widetilde{\mathcal{P}}_d$, there exists a solution to \mathcal{V}_d^U , together with \mathcal{V}_d^D , is feasible to \mathcal{P}_d . That is, if $\mathcal{V}_d^D \in \widetilde{\mathcal{P}}_d$, there must $\exists \mathcal{V}_d^U$ such that $(\mathcal{V}_d^U, \mathcal{V}_d^D) \in \mathcal{P}_d$. The projected feasible region $\widetilde{\boldsymbol{\mathcal{P}}}_d$ for desired variables $\boldsymbol{\mathcal{V}}_d^D$ can be represented as in (28), where $A_{h,i,t}^{\theta}$, $A_{h,i,t}^{P}$, and $A_{h,g,t}^{G}$ are generated coefficients to desired variables $\theta_{i,t}$ and $p_{i,t}$, $\forall i \in \mathcal{I}_d^B$ and $p_{g,t}$; $B_{h,t}$ is the generated constant term; $\mathcal{H}_{d,t}$, indexed by h, collects all constraints generated at hour t.

$$\begin{split} & \sum_{i \in \mathcal{I}_d^B} A_{h,i,t}^{\theta} \cdot \theta_{i,t} + \sum_{i \in \mathcal{I}_d^B} A_{h,i,t}^P \cdot p_{i,t} \\ & + \sum_{g \in \mathcal{G}_d^D} A_{h,g,t}^G \cdot p_{g,t} \le B_{h,t}; \quad h \in \mathcal{H}_{d,t}, \ t \in \mathcal{T} \end{split} \tag{28}$$

The projected feasible region $\widetilde{\boldsymbol{\mathcal{P}}}_d$ of distribution system dshall be prepared by the DSO and submitted to the ISO, together with bids of DERs. Desired variables serve as an interface to describe the interaction of distribution system d with the transmission system. Specifically, variables $\theta_{i,t}$ and $p_{i,t}$ $(i \in \mathbf{J}_d^B)$ are forced equal to their counterparts $\hat{\theta}_{i',t}$ and $\hat{p}_{i',d,t}$ $(i' \in \mathcal{J}_{i,d}^T)$ defined at the transmission side as in (29). This is illustrated in Fig. 2. In addition, energy production costs of DERs shall be added into the objective as in (30). Moreover, the ISO shall include the projected feasible region $\widetilde{\mathcal{P}}_d$ (28) into the energy market model (1)-(12) to represent physical operation limits of distribution system d.

$$\hat{\theta}_{i',t} = \theta_{i,t}; \quad \hat{p}_{i',d,t} = p_{i,t}; \quad i' \in \mathcal{J}_{i,d}^{T}, i \in \mathcal{J}_{d}^{B}, t \in \mathcal{T} \qquad (29)$$

$$\min \sum_{t \in \mathcal{T}} \sum_{g \in \mathcal{G}^{T}} (\hat{C}_{g} \cdot \hat{p}_{g,t} + \widehat{CL}_{g} \cdot \hat{I}_{g,t} + \widehat{SU}_{g} \cdot \hat{Y}_{g,t}) + \sum_{t \in \mathcal{T}} \sum_{d \in \mathcal{D}} \sum_{g \in \mathcal{G}_{d}^{D}} C_{g} \cdot p_{g,t} \qquad (30)$$

After the ISO energy market is cleared, solutions to the desired variables will be sent back to DSOs, based on which, individual DSO can recover feasible solutions to undesired variables according to the original constraints (13)-(25) via a self-scheduling problem.

- C. Further Discussions on the Feasible Region Projection and the Distribution System Integration
- Modeling Unit Commitment Status of DERs: To model unit commitment decisions of DERs, constraints (24)-(25) shall be replaced by (31)-(32).

$$P_g^{LB} \cdot I_{g,t} \le p_{g,t} \le P_g^{UB} \cdot I_{g,t}; \qquad g \in \mathcal{G}_d^D, t \in \mathcal{T}$$

$$Q_g^{LB} \cdot I_{g,t} \le q_{g,t} \le Q_g^{UB} \cdot I_{g,t}; \qquad g \in \mathcal{G}_d^D, t \in \mathcal{T}$$

$$(31)$$

In this case, $I_{a,t}$ is also considered as a desired variable in the feasible region projection, which shall be involved in the objective function (33) to count for no-load and startup costs of DERs. This also extends (28) to (34), where $A_{h,q,t}^{I}$ is generated coefficients to $I_{g,t}$. Startup status indicators $Y_{g,t}$ of DERs can be linked with $I_{q,t}$ via the classic "3-bin" form startup/shutdown constraints similar as (6)-(7). Moreover, other constraints related to ON/OFF status of DERs, such as minimum ON/OFF time constraints (8)-(9), can also be formulated via $I_{g,t}$ and $Y_{g,t}$ as needed.

$$\begin{aligned} \min & \sum_{t \in \mathcal{T}} \sum_{g \in \mathcal{G}^T} (\hat{C}_g \cdot \hat{p}_{g,t} + \widehat{CL}_g \cdot \hat{I}_{g,t} + \widehat{SU}_g \cdot \hat{Y}_{g,t}) + \\ & \sum_{t \in \mathcal{T}} \sum_{d \in \mathcal{D}} \sum_{g \in \mathcal{G}_d^D} (C_g \cdot p_{g,t} + CL_g \cdot I_{g,t} + SU_g \cdot Y_{g,t}) \\ & \sum_{i \in \mathcal{I}_d^B} A_{h,i,t}^{\theta} \cdot \theta_{i,t} + \sum_{i \in \mathcal{I}_d^B} A_{h,i,t}^{P} \cdot p_{i,t} + \sum_{g \in \mathcal{G}_d^D} A_{h,g,t}^{I} \cdot I_{g,t} \\ & + \sum_{g \in \mathcal{G}_d^D} A_{h,g,t}^{G} \cdot p_{g,t} \leq B_{h,t}; \qquad h \in \mathcal{H}_{d,t}, \ t \in \mathcal{T} \end{aligned}$$
(34)

• Computational Complexity of Feasible Region Projection: As filtering strategies can only partially resolve computational issue of the Fourier-Motzkin elimination, we further leverage distinct characters of distribution systems to mitigate computational complexity. Indeed, considering that violations could merely happen on a limited number of lines and buses in distribution systems, not all assets need to be monitored in practice. Therefore, constraints (20)-(21) can be applied only on carefully selected lines and buses, which could further reduce computational burden of the feasible region projection.

We also note that the feasible region projection is conducted offline by DSOs to prepare for the ISO market participation. Thus, constructing the projected feasible region is not a time-critical task for DSOs.

• Implementation of the Feasible Region Projection: Both Gaussian elimination and Fourier-Motzkin elimination involve a series of multiplication and division operations. Implementing these operations via floating-point arithmetic may introduce numerical errors, whose accumulation could further result in numerical issues. Therefore, it is suggested to represent all coefficients in (13)-(25) as fraction numbers, so that floating point arithmetic can be replaced by integer arithmetic to mitigate numerical issues. Importantly, digital lengths of numerators and denominators shall be effectively controlled, so as to ensure calculation accuracy while avoiding trivial calculations of fractions with digital length explosion. An example is that 0.3333332 may be reasonably represented as 1/9 instead of 55555/499996, with negligible accuracy loss.

Various programming languages provide packages and classes to implement fraction number operations, such as *Fraction* in Python and *Sym* in MATLAB, with different computational performance. As a matter of fact, *Fraction* is significantly more computationally efficient than *Sym*. It is also emphasized that a delicate program design and a proper programming language could also dramatically improve the computational performance.

• Advantages of the Proposed Feasible Region Projection Approach: Formulating feasible region (13)-(25) of a distribution system requires detailed network configuration data, including network topology as well as parameters of lines and DERs, while also introducing a complicated power flow model with voltage and reactive power flow variables. Through feasible region projection to convert (13)-(25) into (28), voltage and reactive power flow variables are eliminated, while active power variables of DERs are kept to describe the interaction between distribution and transmission systems, which aligns with the focus of ISO energy market. Constraint (28) is compatible to the ISO energy market model (1)-(12), and can be implemented with limited efforts. Moreover, moving from (13)-(25) to (28), the original coefficients in

(13)-(25) are masked by the new coefficients in (28) that conceal physical meanings, which could also resolve potential data privacy barriers between the ISO and DSOs.

Another prominent advantage of the proposed distribution system integration model lies in that no iterative interaction between the transmission system and distribution systems is required during the market clearing procedure, which is consistent with the current ISO market clearing practice.

In addition, the proposed model is expected to present higher computational performance than the full transmissiondistribution model by directly including the full distribution system model (13)-(25) into the ISO energy market.

D. Data Flow and Further Discussions on the Proposed Approach

The data flow of the proposed approach is shown in Fig. 4. During the ISO energy market bidding phase, a DSO collects the network data and operational limits of DERs to build model (13)-(25), which will be further processed with the feasible region projection approach to generate the projected feasible region $\tilde{\mathcal{P}}_d$. Together with bids from DERs, $\tilde{\mathcal{P}}_d$ is submitted to ISO for being integrated into the ISO energy market model. After the bidding phase is closed, ISO will use DERs' bids and $\tilde{\mathcal{P}}_d$ from the DSOs to clear the energy market. To sum up, on the ISO side, DERs' bids and $\tilde{\mathcal{P}}_d$ from DSOs are required; DSOs require operational limits of DERs, such as P_g^{LB} and P_g^{UB} , and distribution network data, such as $G_{i-i'}$ and $P_{i-i'}^{UB}$, in preparing $\tilde{\mathcal{P}}_d$.

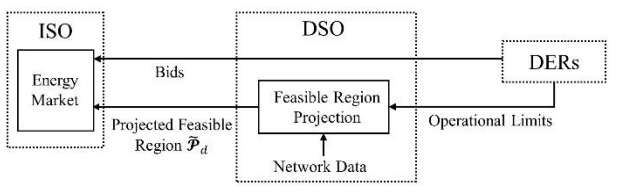


Fig. 4 Bidding process and data flow of the proposed approach

The computational complexity and numerical stability of the feasible region projection approach could be a potential barrier when applying the proposed integration model for large-scale distribution systems. Some of these limitations have been discussed in Section III.C. Besides those, another limitation is that on the transmission side, a voltage phase angle based DC power flow model (2)-(3) is adopted, in which voltage phase angle variables $\hat{\theta}_{i,t}$ are used for the purpose of representing couplings between power injections of distribution systems through multiple interconnection buses. However, as shown in the case study, comparing with the shift factor DC power flow model, this form involves more variables and constraints that could result in a higher computational burden. A special case that all distribution systems are single bus interconnected is also discussed, in which the shift factor based DC power flow model can be adopted without compromising modeling validity.

IV. SPECIAL CONSIDERATION ON DISTRIBUTION SYSTEMS WITH SINGLE INTERCONNECTION BUSES

The integration model discussed above is for general

distribution systems with multiple interconnection buses to the transmission system. In this section, we analyze a special case that each distribution system is connected to the transmission system via a single interconnection bus, to explore its beneficial features in advancing the feasible region projection.

A. Feasible Region Projection of Distribution Systems with Single Interconnection Buses

For the case of multiple interconnection buses, from the prospective of the distribution side, the transmission system is presented as multiple recourses with net power injection $p_{i,t}$ at each interconnection bus i. Critically, $p_{i,t}$ for $i \in \mathcal{J}_d^B$ are electrically coupled. That is, the summation of $p_{i,t}$ is equal to the net load of the distribution system, while values of individual $p_{i,t}$ are determined by physical features of both the transmission and distribution sides. Indeed, this coupling is enforced by constraint (29), requiring $\theta_{i,t}$ equal to $\hat{\theta}_{i',t}$ ($i' \in \mathcal{J}_{i,d}^T$) on individual interconnection buses.

By contrast, in the case of a single interconnection bus as shown in Fig. 5, only one $p_{i,t}$ exists which is solely determined by net load of the distribution side. Thus, $\hat{\theta}_{i',t} = \theta_{i,t}$ ($i' \in \mathcal{J}_{i,d}^{B}$, $i \in \mathcal{J}_{d}^{B}$) could be naturally managed, and $\theta_{i,t}$ ($i \in \mathcal{J}_{d}^{D}/\mathcal{J}_{d}^{B}$) is no longer needed to explicitly simulate the coupling between transmission and distribution systems.

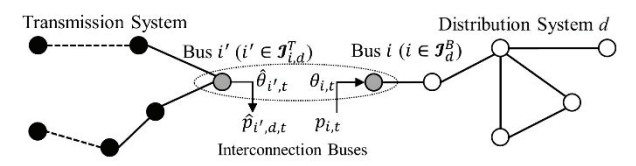


Fig. 5 An illustrative example of a distribution system with a single interconnection bus

To this end, $\theta_{i,t}$ ($i \in \mathcal{I}_d^D/\mathcal{I}_d^B$) can be further classified as undesired variables. Variables in the feasible region \mathcal{P}_d can be split as $\mathcal{V}_d^D = \{p_{i,t}, \forall i \in \mathcal{I}_d^B; p_{g,t}\}$ and all other variables in \mathcal{V}_d^U . That is, all voltage phase angle variables $\theta_{i,t}$ are undesired and will be eliminated. Thereby, the projected feasible region can be represented as in (35), in which $\theta_{i,t}$ is absence comparing with (28).

$$\sum_{i \in \mathcal{I}_{d}^{B}} A_{h,i,t}^{P} \cdot p_{i,t} + \sum_{g \in \mathcal{G}_{d}^{D}} A_{h,g,t}^{G} \cdot p_{g,t} \le B_{h,t};$$

$$h \in \mathcal{H}_{d,t}, \ t \in \mathcal{T}$$

$$(35)$$

By leveraging the fact that $\theta_{i,t}$ are not needed to represent the coupling between transmission and distribution systems with single interconnection buses, the following two strategies are studied to facilitate the feasible region projection process:

- (i) For a distribution system, its interconnection bus is set as the internal reference bus, i.e., voltage phase angle variable $\theta_{i,t}$ for $i \in \mathcal{J}_d^B$ is set as 0 to directly eliminate $\theta_{i,t}$.
- (ii) After *Gaussian elimination*, the remaining variables in inequality constraints are $p_{i,t}$, $p_{g,t}$, and $q_{g,t}$. Leveraging the feature that boundaries of $p_{i,t}$, $p_{g,t}$, and $q_{g,t}$ are known in advance, we propose a boundary filtering strategy to identify inactive constraints with limited computational efforts. That is, for a constraint in the standard " \leq " form, its maximum possible value can be

calculated by substituting the variable associated with a positive/negative coefficient via its upper/lower bound. If strictly less than still holds with the maximum possible value, this constraint is redundant and can be dropped.

The flowchart of the feasible region projection with the embedded boundary filtering strategy is shown in Fig. 6. Specifically, the three filtering strategies can be executed sequentially on individual generated constraints, so that the most computational expensive LP filtering strategy is only applied on a few constraints that pass the first two strategies.

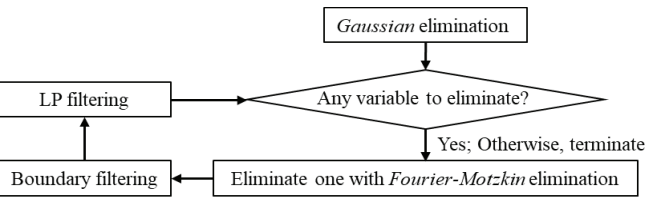


Fig. 6 Flowchart of the feasible region projection with boundary filtering

After the ISO market is cleared, with solutions to desired variables released by the ISO, a DSO can recover feasible solutions to undesired variables via a self-scheduling problem based on (13)-(25). However, the recovered voltage phase angles $\theta_{i,t} \ \forall i \in \mathcal{I}_d^D$ are referred to its own interconnection bus, instead of the reference bus ref of the transmission system. This can be easily fixed by adding the value of $\hat{\theta}_{i',t}$ ($i' \in \mathcal{I}_{i,d}^T$), i.e., voltage phase angle solution of the interconnection bus from the transmission side, to individual $\theta_{i,t}, \ \forall i \in \mathcal{I}_d^D$. After that, all voltage phase angle solutions are referred to the global reference bus ref of the transmission system, and constraint (29) is naturally met.

B. ISO Energy Market Clearing Model with All Distribution Systems Being Single Bus Interconnected

When each primary distribution system is connected to the transmission system via a single interconnection bus, bus voltage angles $\hat{\theta}_{i,t}$ are not needed from the perspective of formulating the coupling of transmission and distribution systems. To this end, the shift factor form, as the common practice of ISOs, can be adopted to build the DC power flow model in the ISO energy market. That is, constraints (2)-(3) can be replaced with (36)-(37), and constraint (12) can be removed. Constraint (36) is the system power balance, and (37) calculates line flow. Indeed, adopting shift factors can reduce the numbers of variables and constraints (i.e., avoid variables $\hat{\theta}_{i,t}$ as well as nodal power balance constraints), with dramatically reduced computational burden.

$$\sum_{g \in \mathcal{G}^T} \hat{p}_{g,t} = \sum_{d \in \mathcal{D}} \sum_{i \in \mathcal{I}_d^B} \hat{p}_{i,d,t} + \sum_{f \in \mathcal{F}^T} \hat{P}_{f,t}; \quad t \in \mathcal{T}$$
(36)
$$\hat{p}_{i-i',t} = \sum_{i'' \in \mathcal{I}^T} \widehat{SF}_{i-i',i''} \cdot \left(\sum_{g \in \mathcal{G}_{i''}^T} \hat{p}_{g,t} - \sum_{d \in \mathcal{D}_{i''}} \hat{p}_{i'',d,t} - \sum_{f \in \mathcal{F}_{i,l'}^T} \hat{P}_{f,t} \right); \quad i - i' \in \mathcal{L}^T, t \in \mathcal{T}$$
(37)

V. CASE STUDIES

In this section, efficacy of the proposed method is illustrated via multiple case studies. In addition, an illustrative example is included in the Appendix to show the details of how to apply the proposed method.

A. Test System Setup and Case Design

The 1888-bus transmission system from the MATPOWER library, together with multiple interconnected distribution systems, is used to evaluate the proposed approach in terms of solution quality and computational performance. Each of the distribution systems is connected to the transmission system through one or two interconnection buses, referred to as Type DS-1 and Type DS-2 distribution systems. Modified based on the 33-bus distribution system, both types of distribution system include 8 DERs and 34 distribution lines that form a looped topology. Distribution systems of the same type are identical except for their interconnection buses.

In each distribution system, power flows of all 34 lines are monitored via constraint (20), and voltage magnitudes of all 33 buses are monitored via constraint (21), with V_i^{LB}/V_i^{UB} of 0.95p.u./1.05p.u.. In addition, electricity bidding prices of DERs are set to be generally lower than those of thermal units in the transmission system. The detail system data can be found in [22].

Four cases are studied, as summarized in Table I. *Cases 1-3* respectively include 5, 10, and 15 DS-2 distribution systems; *Case 4* includes 15 DS-1 distribution systems.

TABLE I. SUMMARY OF CASES

Case-	Distribution systems		Calvina madala	
Case Nu	Number	Type	Solving models	
1	5	DS-2	Full Model; Full Model ^{UC}	
2	10	DS-2	Proposed Model; Proposed Model ^{UC}	
3	15	DS-2	Simplified Model	
1	15	DS-1	Full Model; Full Model ^{SF}	
4	13	D3-1	Proposed Model ^{SF}	

- In *Cases 1-3*, the following three distribution system integration models are studied:
 - o *Full Model*: Feasible operation region (13)-(25) and coupling constraint (29).
 - o *Proposed Model*: Feasible operation region projection (28) and coupling constraint (29).
 - o Simplified Model: Constraints (24) and (38). For $i' \in \mathcal{J}_{i,d}^T$, $\hat{p}_{i',d,t}$ is limited in the range of $[P_i^{LB}, P_i^{UB}]$.

$$\sum_{g \in \mathcal{G}_d^D} p_{g,t} + \sum_{i \in \mathcal{I}_d^B} \sum_{i' \in \mathcal{I}_{i,d}^T} \hat{p}_{i',d,t} = \sum_{f \in \mathcal{F}_d^D} P_{f,t}; \quad t \in \mathcal{T} \quad (38)$$

Simplified Model represents ISO's current practice that DERs in distribution systems are allowed to directly bid at the interconnection buses (i.e., distribution network constraints are neglected, and power exchange between the transmission and distribution systems through multiple interconnection buses are not restricted by physical laws of the distribution network). In addition, Full Model and Proposed Model are further extended to consider unit commitment status of DERs by replacing (24)-(25) via (31)-(32) and replacing (28) via (34). These two variations are referred to as Full Model^{UC} and Proposed Model^{UC}.

• In Case 4, as all distribution systems are single bus interconnected, the ISO energy market model can be formulated via shift factors as follows:

Objective: (1)

Subject to: (4)-(11) and (36)-(37)

To this end, two additional models are studied in Case 4,

which are referred to as *Full Model*^{SF} and *Proposed Model*^{SF}:

o *Full Model*^{SF}: Feasible region (13)-(25) as well as coupling constraint (39).

$$\theta_{i,t} = 0; \ \hat{p}_{i',d,t} = p_{i,t} \qquad i' \in \mathcal{J}_{i,d}^T, i \in \mathcal{J}_d^B, t \in \mathcal{T}$$
 (39)
 $\circ Proposed Model^{SF}$: Feasible region projection (35)
and coupling constraint (39).

The feasible region projection method, including *Gaussian elimination*, *Fourier-Motzkin elimination*, and the embedded filtering strategies, is implemented in Python. *Fraction* package is used to enable fraction calculations. The boundary filtering strategy is applied on both types of distribution systems. For $\theta_{i,t}$ ($i \in \mathcal{I}_d^B$), we set the range as $[-35^\circ, +35^\circ]$. All derived optimization problems are MILP models, which are implemented in MATLAB and solved by Gurobi 9.0.0. All numerical simulations are conducted on a PC with i7-3.6GHz CPU and 16GB RAM.

B. Case Study Analysis

B.1 Comparison of Various Models in Cases 1-3

- Performance of the Feasible Region Projection: For a DS-2 distribution system studied in Cases 1-3, at hour t=1 for instance, it takes 125.56 seconds for the projection process to generate 74 constraints of (28). When unit commitment status of DERs is further considered, at hour t=1, 89 constraints of (34) are generated in 185.51 seconds. It is worthwhile to emphasize that feasible region projections of individual hours can be implemented parallelly.
- Comparison of Full Model and Proposed Model: Market clearing results of Full Model and Proposed Model are compared in Table II. All the cases are solved to zero MIP gap for fair comparison.

TABLE II. PERFORMANCE OF FULL MODEL AND PROPOSED MODEL

Case	Full Model		Proposed Model	
Case	Objective (\$)	Solving time (s)	Objective (\$)	Solving time (s)
Case 1	32,201,361.39	105.96	32,201,361.39	72.86
Case 2	32,204,065.73	145.35	32,204,065.73	77.31
Case 3	32,206,766.45	179.92	32,206,766.45	103.29

From Table II we can observe that, the two models derive identical objectives in each case, which verifies the ability of *Proposed Model* in fully capturing the impacts of physical and economic features of distribution systems in the ISO market clearing. In terms of calculation performance, computational burden increases with the increasing number of distribution systems. Indeed, *Proposed Model* significantly outperforms *Full Model* in all three cases, especially when more distribution systems are connected. This shows that the proposed model presents computational efficiency, while showing the other advantages as discussed in Section III.C.

In addition, the modeling accuracy of the distribution system model is verified by comparing voltages recovered from the linear distribution system model (13)-(25) and those from solving an AC power flow problem with respect to dispatches of DERs obtained from the ISO energy market clearing results. The comparison of the two voltage profiles shows an average error of 0.15% and the maximum error of 0.44% on voltage magnitudes. This indicates an acceptable

performance of the adopted model in terms of accuracy.

Comparison of Proposed Model and Simplified Model: We further compare Proposed Model and Simplified Model in terms of physical feasibility against distribution system constraints (13)-(25). With an ISO market clearing result to desired variables \mathcal{V}_d^D from Proposed Model or Simplified Model, we try to recover a feasible solution to (13)-(25), if deemed feasible. Table III shows that, feasible solutions to distribution systems can always be recovered with results from Proposed Model in all three cases, while infeasibility consistently occurs with Simplified Model. This verifies effectiveness of the feasible region projection in respecting distribution systems' internal physical limits, which shows the necessity of considering internal physical limits of distribution systems in ISO energy market clearing. This also explains why Simplified Model derives lower objective values and shorter solving time than Proposed Model.

We use Case 1 as an example to further analyze effects of the proposed approach in delivering feasible solutions to the distribution systems. With results from *Proposed Model*, the recovered bus voltage profile in one distribution system at hour 12 is shown in Fig. 7. It can be seen that voltage at bus 18 reaches the upper limit (i.e., $V_i^{UB}=1.05$). That is, constraint (21) is binding, which is mainly caused by active power injections of DERs connected at this bus. This verifies the effectiveness of constraint (28) in respecting distribution systems' internal limits. On the other hand, no feasible solution to the distribution system can be recovered based on the results from Simplified Model. In recognizing the binding status of voltage constraints and the ignorance of couplings on $p_{i,t}$, if constraints (21) for buses 17 and 18 are remove and slack variables are added in the power balance constraints, we could recover a solution to the distribution system. Recovered voltage profile is compared in Fig. 7, which shows that voltage of bus 18 is 1.0603p.u., violating the upper bound. Indeed, values of slack variables in power balance constraints of the two interconnection buses are both non-zeros (i.e., one is -4.16MW and the other is +4.16MW). That is, net power injections of the two interconnection buses will deviate -4.16MW and +4.16MW from the results cleared in the ISO market, in order to align with the given voltage phase angles of interconnection buses.

TABLE III. COMPARISON OF PROPOSED MODEL AND SIMPLIFIED MODEL

1711	TABLE III. COM ANGOLI OF TROPOSED MODEL AND DIM EN IED MODEL				
Proposed Model		Simplified Model			
Case	Feasibility to (13)-(25)	Objective (\$)	Solving time (s)	Feasibility to (13)-(25)	
Case 1	Yes	32,201,250.62	68.21	No	
Case 2	Yes	32,203,841.88	69.28	No	
Case 3	Yes	32,206,433.34	67.22	No	

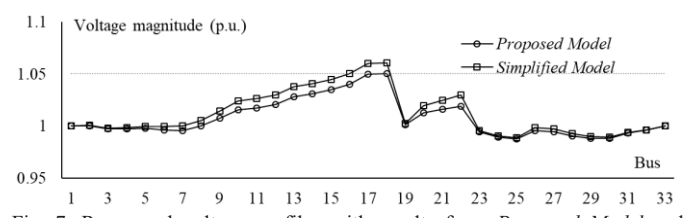


Fig. 7. Recovered voltage profiles with results from *Proposed Model* and *Simplified Model*

Analyze the Effect When Unit Commitment Status of DERs Is Considered: Market clearing results of Full Model^{UC} and Proposed Model^{UC} are compared in Table IV. The MIP gap threshold is set as 0.01%, in observing that seeking zero MIP gap solutions would cause trivial ON/OFF status switching on DERs but dramatically increase the solving time for both models. Indeed, similar observations as in Table II can be made, in terms of solution quality and computational performance. The slight difference in objectives of the two models in Case 2 and Case 3 are caused by non-zero MIP gap. In addition, comparing with Table II, higher objectives are observed because no-load costs of DERs are considered. Although avoiding seeking zero MIP gap solutions contributes to lower computational time of Case 1 and Case 2 in Table IV, it also shows that considering unit commitment of DERs does not necessarily lead to higher computational burden.

TABLE IV. PERFORMANCE OF THE FULL MODEL UC AND PROPOSED MODEL UC

Case		Full Model ^{UC}		Proposed Model ^{UC}	
Cas	6	Objective (\$)	Solving time (s)	Objective (\$)	Solving time (s)
Case	1	32,203,913.95	102.16	32,203,913.95	64.02
Case	2	32,208,873.36	138.85	32,208,880.51	70.72
Case	3	32,213,981.24	194.52	32,213,974.09	118.96

B.2 Analysis on Type DS-1 Distribution Systems in Case 4

In Case 4, all distribution systems are Type DS-1, and $\theta_{i,t}$ is not needed to formulate the coupling between transmission and distribution systems. As expected, the projected feasible region has fewer constraints as compared to Type DS-2. For instance, at hour t=1, constraint (35) contains 19 constraints after final filtering, as compared to 74 constraints from (28).

Market clearing results from *Full Model*, *Full Model*^{SF}, and *Proposed Model*^{SF} are compared in Table V. It can be seen from Table V that the three models yield identical objectives, which indicates they all can correctly capture the physical limits and economic features of distribution systems. However, *Full Model*^{SF} and *Proposed Model*^{SF} dramatically outperform *Full Model* in terms of computational time, which shows advantage of the shift factor-based market clearing model, i.e., much fewer variables and constraints. Moreover, computational time of *Proposed Model*^{SF} is slightly shorter than that of *Full Model*^{SF}.

In addition, from *Full Model*, voltage phase angles of buses in distribution system can be obtained directly. For instance, $\theta_{i,t}$ of bus 1 and bus 33 at hour t=1 are -10.42° and -9.76°. In comparison, the other two models will have to conduct additional calculations to calculate voltage phase angles of distribution systems. The additional calculations involve solving equations (2)-(3) with known dispatches and then recovering the undesired variables.

TABLE V. PERFORMANCE OF THREE MODELS IN CASE 4

Model	Full Model	Full Model ^{SF}	Proposed Model ^{SF}
Objective (\$)	32,205,601.35	32,205,601.35	32,205,601.35
Solving time (seconds)	135.70	28.91	24.58

VI. CONCLUSION

This paper proposes a feasible region projection-based approach for integrating DER-penetrated primary distribution

systems into the ISO energy market. The proposed model is practically applicable in the current ISO energy market platform. It does not require ISO collecting configuration details of or conducting an iterative procedure with distribution systems. Case studies illustrate that the proposed model can fully capture economic features of distribution systems and respect their internal physical limits, while is computationally more efficient than the full model by directly including the exhaustive formulation of distribution systems.

APPENDIX

An illustrative example shown in Fig. 8 is used to further illustrate how the proposed approach works. It contains one distribution system, which is interconnected with the transmission system through two interconnection buses. After duplicating the interconnection buses, the system can be decoupled as the transmission system and the distribution system (i.e., d=1), as shown in Fig. 9. For the distribution system, its feasible operation region can be formulated following (13)-(25), while variables $\theta_{4,t}$, $\theta_{5,t}$, $p_{4,t}$, $p_{5,t}$, and $p_{a=1,t}$ are the desired variables. By applying the feasible region projection approach, (13)-(25) turn to (40) that will be integrated into the ISO energy market model, together with constraints (41)-(42) that build up the linkage between variables of the duplicated interconnection buses. In the objective, $C_{g=1} \cdot p_{g=1,t}$ is included, representing the energy cost of DER g=1 in the distribution system.

$$\begin{split} A_{h,4,t}^{\theta} \cdot \theta_{4,t} + A_{h,5,t}^{\theta} \cdot \theta_{5,t} + A_{h,4,t}^{P} \cdot p_{4,t} + A_{h,5,t}^{P} \cdot p_{5,t} \\ + A_{h,g=1,t}^{G} \cdot p_{g=1,t} \leq B_{h,t}; \quad h \in \mathcal{H}_{d=1,t}, \ t \in \mathcal{T} \\ \hat{\theta}_{3,t} = \theta_{4,t}; \quad \hat{\theta}_{4,t} = \theta_{5,t}; \qquad \qquad t \in \mathcal{T} \\ \hat{p}_{3,1,t} = p_{4,t}; \quad \hat{p}_{4,1,t} = p_{5,t}; \qquad \qquad t \in \mathcal{T} \end{split} \tag{41}$$

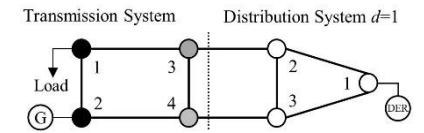


Fig. 8. An illustrative example

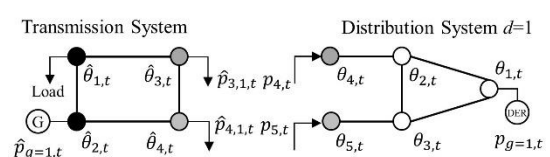


Fig. 9. The example system after duplicating the interconnection buses

REFERENCES

- Department of Energy, "Quadrennial energy review transforming the nation's electricity system: the second installment of the QER," Jan. 2017. [Online] Available: https://www.energy.gov/policy/initiatives/ quadrennial-energy-review-qer/quadrennial-energy-review-second-instal lment.
- [2] W. Hogan, "Electricity markets and the clean power plan," The Electricity Journal, vol. 28, no. 9, pp. 9-32, Nov. 2015.
- [3] R.A. Verzijlbergh, L.J.D. Vries, and Z. Lukszo, "Renewable energy sources and responsive demand. do we need congestion management in the distribution grid?" *IEEE Trans. Power Syst.*, vol. 29, no. 5, pp. 2119-2128, Sept. 2014.
- [4] S. Y. Hadusha and L. Meeus, "DSO-TSO cooperation issues and solutions for distribution grid congestion management," *Energy Policy*,

- vol. 120, pp. 610-621, Sep. 2018.
- [5] A. Keane, L. F. Ochoa, E. Vittal, et al, "Enhanced utilization of voltage control resources with distributed generation," *IEEE Trans. Power Syst.*, vol. 26, no. 1, pp. 252-260, May 2011.
- [6] NYISO, "Distributed energy resources roadmap for New York's wholesale electricity market," Jan. 2017. [Online] Available: https://www.nyiso.com/documents/20142/2261851/2017-Distributed-Energy-Resources-Roadmap.pdf.
- [7] M. Birk, J. Chaves-Ávila, T. Gómez, and R. Tabors, "TSO/DSO coordination in a context of distributed energy resource penetration," Oct. 2017. [Online] Available: http://ceepr.mit.edu/files/papers/2017-017.pdf.
- [8] A. Vicente-Pastor, J. Nieto-Martin, D.W. Bunn, and A. Laur, "Evaluation of flexibility markets for Retailer—DSO—TSO coordination," *IEEE Trans. Power Syst.*, vol. 34, no. 3, pp. 2003-2012, May 2019.
- [9] M. Bragin and Y. Dvorkin, "Toward coordinated transmission and distribution operations," *IEEE Power & Energy Society General Meeting (PESGM)*, Portland, OR, USA, Aug. 2018.
- [10] H. Wu, M. Shahidehpour, A. Alabdulwahab, and A. Abusorrah, "Demand response exchange day-ahead scheduling with variable renewable generation," *IEEE Trans. on Sustain. Energy*, vol. 6, no. 2, pp. 516-525, Apr. 2015.
- [11] A. Daraeepour, S. J. Kazempour, D. Patiño-Echeverri and A. J. Conejo, "Strategic demand-side response to wind power integration," IEEE Trans. *Power Syst.*, vol. 31, no. 5, pp. 3495-3505, Sep. 2016.
- [12] A. Safdarian, M. Fotuhi-Firuzabad, M. Lehtonen, and F. Aminifar, "Optimal electricity procurement in smart grids with autonomous distributed energy resources," *IEEE Trans. on Smart Grid*, vol. 6, no. 6, pp. 2795-2984, Nov. 2015.
- [13] A. Saint-Pierre and P. Mancarella, "Active distribution system management: a dual-horizon scheduling framework for DSO/TSO interface under uncertainty," *IEEE Trans. on Smart Grid*, vol. 8, no. 5, pp. 2186-2197, Sep. 2017.
- [14] A. Papavasiliou and I. Mezghani, "Coordination schemes for the integration of transmission and distribution system operations," *Power Systems Computation Conference (PSCC)*, Dublin, Ireland, Jun. 2018.
- [15] Z. Yuan and M. R. Hesamzadeh, "Hierarchical coordination of TSO-DSO economic dispatch considering large-scale integration of distributed energy resources," *Appl. Energy*, vol. 195, no. 2, pp. 600-615, Jun. 2017.
- [16] J. Silva, J. Sumaili, R.J. Bessa, et al, "Estimating the active and reactive power flexibility area at the TSO-DSO interface," *IEEE Trans. Power Syst.*, vol. 33, no. 5, pp. 4741-4750, Sep. 2018.
- [17] Z. Yang, H. Zhong, Q. Xia, and C. Kang, "Solving OPF using linear approximations: fundamental analysis and numerical demonstration", IET Gener., Transm. Distrib., vol. 11, no. 17, pp. 4115-4125, Dec. 2017.
- [18] G. Strang, Linear Algebra and Its Application, Brooks/Cole, India, 2005.
- [19] J. L. Imbert, "Fourier's elimination: Which to choose?" in Proc. PPCP, pp. 1-13, 1993.
- [20] A. Abiri-Jahromi, and F. Bouffard, "On the Loadability sets of power systems--Part II: minimal representations," *IEEE Trans. Power Syst.*, vol. 32, no. 1, pp. 146-156, Jan. 2017.
- [21] S. Paulraj and P. Sumathi "A comparative study of redundant constraints identification methods in linear programming problems," *Mathematical Problems in Engineering*, vol. 2010, pp. 1-16, 2010.
- [22] https://sites.google.com/site/leiwupes/data/TD Projection.zip.

BIOGRAPHIES

Yikui Liu (S'15) received the B.S. degree in electrical engineering and automation from Nanjing Institute of Technology, China, in 2012, the M.S. degree in power system and automation from Sichuan University, China, in 2015, and the Ph.D. degree in electrical and computer engineering from Stevens Institute of Technology, USA, in 2020. His research interests include power market and OPF in distribution system.

Lei Wu (SM'13) received the B.S. degree in electrical engineering and the M.S. degree in systems engineering from Xi'an Jiaotong University, Xi'an, China, in 2001 and 2004, respectively, and the Ph.D. degree in electrical engineering from Illinois Institute of Technology (IIT), Chicago, IL, USA, in 2008.

From 2008 to 2010, he was a Senior Research Associate with the Robert W. Galvin Center for Electricity Innovation, IIT. He was a summer Visiting Faculty at NYISO in 2012. He was a Professor with the Electrical and Computer Engineering Department, Clarkson University, Potsdam, NY, USA, till 2018. He is currently a Professor with the Electrical and Computer Engineering Department, Stevens Institute of Technology, Hoboken, NJ, USA. His research interests include power systems operation and planning, energy economics, and community resilience microgrid.

Yonghong Chen (SM'12) received the B.S. degree from Southeast University, Nanjing, China, the M.S. degree from Nanjing Automation Research Institute, China, and the Ph.D. degree from Washington State University, Pullman, WA, USA, all in electrical engineering. She also received the M.B.A. degree from Indiana University, Kelly School of Business, Indianapolis, IN, USA. She is currently a Consulting Advisor at MISO. In this role, she focuses on R&D to address challenges on market design and market clearing system. Before joining MISO in 2002, she worked with GridSouth Transco LLC and Nanjing Automation Research Institute.

Jie Li (M'14) received the B.S. degree in information engineering from Xi'an Jiaotong University in 2003 and the M.S. degree in system engineering from Xi'an Jiaotong University, China in 2006, and the Ph.D. degree from the Illinois Institute of Technology (IIT), Chicago, in 2012.

From 2006 to 2008, she was a Research Engineer with IBM China Research Lab. From 2012 to 2013, she was a Power System Application Engineer with GE Energy Consulting. She was an Assistant Professor with the Electrical and Computer Engineering Department, Clarkson University, Potsdam, NY, USA, during 2014 to 2019. She is currently an Associate Professor with the Electrical and Computer Engineering Department, Rowan University, Glassboro, NJ, USA. Her research interests include power systems restructuring and bidding strategy.